# Supplemental Material for Quantum-Limited Mirror-Motion Estimation

Kohjiro Iwasawa,[1] Kenzo Makino,[1] Hidehiro Yonezawa,[1,*] Mankei Tsang,[2,3] Aleksandar Davidovic,[4] Elanor Huntington,[4,5] and Akira Furusawa[1,†]

[1]*Department of Applied Physics, School of Engineering, The University of Tokyo, 7-3-1 Hongo, Bunkyo-ku, Tokyo 113-8656, Japan*
[2]*Department of Electrical and Computer Engineering, National University of Singapore, 4 Engineering Drive 3, Singapore 117583*
[3]*Department of Physics, National University of Singapore, 2 Science Drive 3, Singapore 117551*
[4]*School of Engineering and Information Technology, The University of New South Wales, Canberra 2600, ACT, Australia*
[5]*Centre for Quantum Computation and Communication Technology, Australian Research Council*

## I. EXPERIMENTAL DETAILS

In this section, we will describe the experimental details. Figure 1 shows our experimental setup [1]. A continuous-wave Titanium Sapphire laser was used as a light source at 860 nm. Phase squeezed states were generated by an optical parametric oscillator (OPO) of a bow-tie shaped configuration with a periodically polled $KTiOPO_4$ crystal as a nonlinear optical medium [2]. The OPO was driven below threshold by a 430 nm pump beam, generated by another bow-tie shaped cavity that contains a $KNbO_3$ crystal. The free spectral range and the half width at half maximum of the OPO were 1 GHz and 13 MHz respectively. Optical sidebands at $\pm$ 5 MHz were used as a carrier beam generated with acousto-optic modulators [1, 3]. Note that these optical sidebands are within the OPO's bandwidth. To avoid experimental complexities, the pump power was fixed to 80 mW giving squeezing and anti-squeezing levels of $-3.62 \pm 0.26$ dB and $6.00 \pm 0.15$ dB respectively. The effective squeezing factor, $\bar{R}_{\rm sq}$, varied from $-3.28$ dB to $-3.48$ dB according to the probe amplitude. Note that $\bar{R}_{\rm sq}$ takes into account of the anti-squeezing quadratures mixing in the measurement, which cannot be neglected for relatively high squeezing levels. It is a trade-off between enhancement from the squeezed quadratures and degradation from the anti-squeezed quadratures, revealing an optimal squeezing level [1]. The optimal squeezing level differs for each amplitude $|\alpha|$, but the difference is minor for our experimental conditions. Since the generated phase squeezed state becomes less robust for higher pumping levels due to the complex locking system, we chose a slightly lower pumping level and did not change it for each $|\alpha|$. For comparison to phase squeezed states, we also used coherent states as a probe by simply blocking the pump beam.

The mirror mounted on a piezoelectric transducer (PZT) was driven by a signal that follows the Ornstein-Uhlenbeck process. This signal was generated with a random signal generator followed by a low-pass filter with a cutoff frequency of $\lambda = 5.84 \times 10^4$ rad/s.

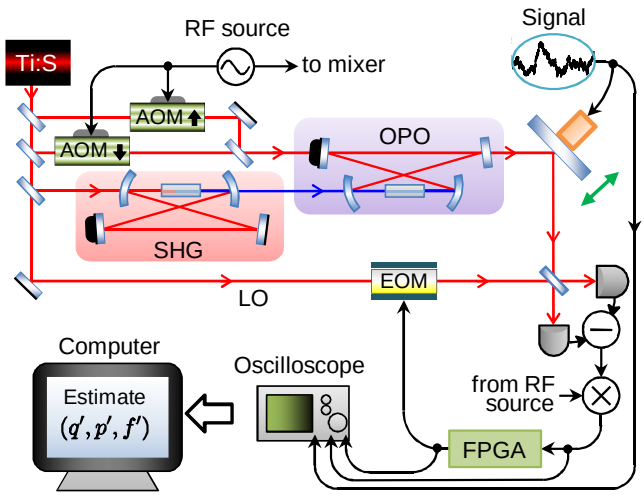


FIG. 1: Experimental setup. Ti:S: Titanium Sapphire laser, LO: Local Oscillator, RF: Radio Frequency, AOM: Acousto-Optic Modulator, EOM: Electro-Optic Modulator, SHG: Second Harmonic Generator, OPO: Optical Parametric Oscillator, FPGA: Field Programmable Gate Array.

A fraction of the laser beam was used as a local oscillator (LO) beam which was passed through a spatial-mode cleaning cavity (not shown in Fig. 1) to increase mode matching with the probe beam. The probe beam and the LO beam are optically mixed with 1:1 beam splitter for homodyne detection. The efficiency of the detection is shown in Table I. The homodyne output was demodulated and recorded with an oscilloscope for post processing.

In the feedback loop, the LO phase is modulated according to the estimated phase. The modulation was performed with a waveguide type electro-optic modulator (EOM). The real-time phase estimate used for feedback was processed with a field programmable gate array (FPGA). The delay of our implemented feedback filter was around 400 ns, which is small enough for our current experimental parameters. Note that we have an-

*Electronic address: yonezawa@ap.t.u-tokyo.ac.jp
†Electronic address: akiraf@ap.t.u-tokyo.ac.jp

TABLE I: Efficiency of the detection.

| | |
|---|---|
| Photo diode quantum efficiency | 0.99 |
| Interference efficiency (Visibility) | 0.965 (0.982) |
| Propagation efficiency | 0.981 |
| Electrical circuit efficiency (Clearance) | 0.924 (11.2 dB) |
| Overall efficiency | 0.871 |

other low-gain, low-frequency feedback loop to prevent environmental phase drifting.

## II. MODELING THE MIRROR MOTION

In this section, we will explain modeling the mirror motion. First, we will consider how to evaluate mass of a PZT-mounted mirror. Then, we will explain transfer function of the PZT-mounted mirror, and the evaluation of *true* signals to be estimated. Finally we will describe the mirror motion functions.

### A. Mass of a mirror attached to a PZT

In our experiment, a multilayer PZT (AE0203D04F, NEC/Tokin) of 3.5 mm×4.5 mm×5.0 mm in size weighing 0.432 g was used. A mirror, 12.7 mm in diameter, 1.5 mm in thickness, weighing 0.444 g was attached to the PZT with an epoxy-based adhesive. The mass of the mirror attached to the PZT was evaluated as follows.

Let the mass of the PZT and mirror be $M_{\rm p}$ and $M_{\rm m}$, respectively. Assume that the mass of the PZT is uniform, and that the displacement is proportional at all points,

$$\Delta l = \frac{l}{L_0}\Delta L. \tag{1}$$

Here, the original length of the PZT is $L_0$, the overall displacement is $\Delta L$, and the displacement at point $l$ ($0 \le l \le L_0$) is $\Delta l$. Then, the kinetic energy may be calculated as

$$\begin{aligned} E &= \frac{1}{2}M_{\rm m}\left[\frac{d}{dt}(\Delta L)\right]^2 + \int_0^{L_0} dx \frac{1}{2}\frac{M_{\rm p}}{L_0}\left[\frac{d}{dt}(\Delta l)\right]^2 \\ &= \frac{1}{2}\left(M_{\rm m} + \frac{1}{3}M_{\rm p}\right)\left[\frac{d}{dt}(\Delta L)\right]^2. \end{aligned} \tag{2}$$

Hence, we assume that $m = M_{\rm m} + M_{\rm p}/3 = (0.444 + 0.432/3)$ g $= 5.88 \times 10^{-4}$ kg.

### B. Transfer function of the PZT-mounted mirror

Next, we will focus on modeling the transfer function of the PZT-mounted mirror. The mass-spring-damper model is referred to as the *nominal model*, which is a simplified model that describes the essence of the targeted system. On the other hand, a model which best describes the targeted system is referred to as the *detailed model*. The detailed model would be the closest measurable model of the targeted system. We used this detailed model to construct optimal filters and calculate the QCRBs, while we used the nominal model to realize real-time feedback control.

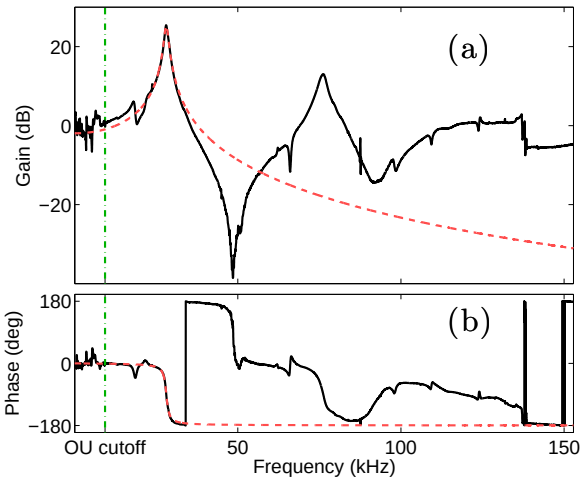


FIG. 2: Transfer functions of the PZT-mounted mirror, gain (a) and phase (b). Black solid lines show the measured transfer function $T_0(\omega)$ referred to as the detailed model. Red dashed lines show the fitted transfer function of the mass-spring-damper system $T_0^{\rm nom}(\omega)$ referred to as the nominal model. The green dot-dashed line shows the cutoff frequency, $\lambda/2\pi$, of the Ornstein-Uhlenbeck (OU) process used in the experiment.

We used a Mach-Zehnder interferometer and a network analyzer to measure the transfer function of the PZT-mounted mirror, $T_0(\omega)$, referred to as the detailed model. The black solid lines in Fig. 2 show the measured results. The red dashed lines in Fig. 2 show the fitted transfer function of the nominal model $T_0^{\rm nom}(\omega) \propto 1/\left(-m\omega^2 + im\omega\gamma + m\Omega^2\right)$ where $\gamma$ is the damping coefficient and $\Omega$ is the mechanical resonant frequency. The fitted parameters were $\Omega = 1.76 \times 10^5$ rad/s and $\gamma = 7.66 \times 10^3$ rad/s.

Note that the external force driving the mirror is generated according to the Ornstein-Uhlenbeck process. The cutoff frequency of this process was set to $\lambda = 5.84 \times 10^4$ rad/s, which is indicated as a green dot-dashed line in Fig. 2. The nominal model is good enough to construct the real-time feedback filter for the experimental conditions.

### C. Evaluation of true signals

In order to evaluate estimation errors, we need to know the *true* position, momentum and external force that are to be estimated (referred to as the target position, target momentum, and target force). We use the full range of the detailed model $T_0(\omega)$ to calculate these target position $q$, momentum $p$, and external force $f$. In the mirror motion estimation experiment, we record the voltage $V(t)$ that drives the PZT-mounted mirror. From $V(t)$, $T_0(\omega)$, and the sensitivity of the photo detector $G = 6.96 \times 10^7$ V/m, we calculate the target position as

$$q(t) = \mathcal{F}^{-1}\left[\frac{T_0(\omega)}{G}\mathcal{F}[V(t)]\right], \tag{3}$$

where $\mathcal{F}$ ($\mathcal{F}^{-1}$) denotes the (inverse) Fourier transform. We use this result to calculate the target momentum,

$$p(t) = m\frac{d}{dt}q(t). \tag{4}$$

The voltage applied to the PZT-mounted mirror is within the linear response range so that the target force may be calculated as

$$f(t) = \beta V(t), \tag{5}$$

where $\beta = 2.04 \times 10^{-1}$ N/V.

### D. Mirror motion functions

Mirror motion functions $g_{ij}(\omega)$ $(i, j = q, p, f, \varphi)$ are defined such as $\tilde{q}(\omega) = g_{qf}(\omega)\tilde{f}(\omega)$ ($i = q$ and $j = f$) where a tilde indicates the Fourier transform. The mirror motion functions are necessary to derive the optimal filters and the QCRBs. Note that the definition leads to $g_{ij}(\omega)g_{jk}(\omega) = g_{ik}(\omega)$ and $[g_{ij}(\omega)]^{-1} = g_{ji}(\omega)$.

From Eqs. (3) and (5), the function $g_{qf}(\omega)$ is given as,

$$g_{qf}(\omega) = \frac{T_0(\omega)}{G\beta}. \tag{6}$$

As denoted in the main text, the phase shift of the probe beam is proportional to the position shift as $\varphi(t) = (2k_0 \cos\theta)q(t)$. Then, the other relevant mirror motion functions are derived as follows:

$$g_{\varphi q}(\omega) = 2k_0 \cos\theta, \tag{7}$$

$$g_{\varphi p}(\omega) = g_{\varphi q}(\omega)g_{qp}(\omega) = \frac{2k_0 \cos\theta}{im\omega}, \tag{8}$$

$$g_{\varphi f}(\omega) = g_{\varphi q}(\omega)g_{qf}(\omega) = 2k_0 \cos\theta \frac{T_0(\omega)}{G\beta}, \tag{9}$$

where we use $g_{qp}(\omega) = 1/(im\omega)$.

## III. OPTIMAL LINEAR FILTER AND LEAST MEAN SQUARE ERROR

In this section, we derive the optimal linear filters which minimize mean square errors (MSEs) [4]. We will explain the position estimate $q'(t)$ and the least position MSE $\Pi_q^{\min}$ as an example. The estimates and MSEs for momentum and force can be derived similarly.

First, let's consider the normalized output of the homodyne detection [1, 5],

$$\eta(t) = \sin[\varphi(t) - \varphi'(t)] + \frac{v(t)}{2|\alpha|}\sqrt{R_{\rm sq}(t)}, \tag{10}$$

$$R_{\rm sq}(t) = \sin^2[\varphi(t) - \varphi'(t)]e^{2r_{\rm p}} + \cos^2[\varphi(t) - \varphi'(t)]e^{-2r_{\rm m}}. \tag{11}$$

Here $r_{\rm m}$ ($r_{\rm p}$) is the squeezing (anti-squeezing) parameter ($r_{\rm p} \geq r_{\rm m} \geq 0$), $|\alpha|$ is the coherent amplitude of the probe beam, $v(t)$ denotes white Gaussian noise with a flat spectral density of 1, and $\varphi'(t)$ is a real-time phase estimate used for the feedback control. This homodyne output can also be applied to coherent states by simply putting $R_{\rm sq} = 1$. Following the quadratic approximation shown in Ref. [1] gives a good approximation of the homodyne output as

$$\eta(t) \simeq \varphi(t) - \varphi'(t) + z(t). \tag{12}$$

Here, $z(t)$ is a white Gaussian noise as,

$$\langle z(t)\rangle = 0, \tag{13}$$

$$\langle z(t)z(\tau)\rangle = \frac{\bar{R}_{\rm sq}}{4|\alpha|^2}\delta(t-\tau), \tag{14}$$

$$\bar{R}_{\rm sq} = \sigma_\varphi^2 e^{2r_{\rm p}} + (1-\sigma_\varphi^2)e^{-2r_{\rm m}}, \tag{15}$$

$$\sigma_\varphi^2 = \langle[\varphi(t) - \varphi'(t)]^2\rangle. \tag{16}$$

$\bar{R}_{\rm sq}$ is called the *effective squeezing factor* [1], which takes into account the anti-squeezed amplitude quadrature as well as the squeezed phase quadrature.

By adding the real-time phase estimate $\varphi'(t)$ (which is measured in the experiment as well as $\eta(t)$) to $\eta(t)$, we obtain the (modified) measurement result $y(t)$,

$$y(t) = \eta(t) + \varphi'(t) \simeq \varphi(t) + z(t). \tag{17}$$

The linear estimate of position, $q'(t)$, is given as a weighted sum of this $y(t)$,

$$q'(t) = \int_{-\infty}^{+\infty} d\tau J_q(t-\tau)y(\tau), \tag{18}$$

where $J_q(t)$ is a linear position filter. Fourier transform of the estimate is calculated as,

$$\begin{aligned}\tilde{q}'(\omega) =& \tilde{J}_q(\omega)\tilde{y}(\omega) = \tilde{J}_q(\omega)\left[\tilde{\varphi}(\omega) + \tilde{z}(\omega)\right] \\ =& \tilde{J}_q(\omega)\left[g_{\varphi q}(\omega)\tilde{q}(\omega) + \tilde{z}(\omega)\right].\end{aligned} \tag{19}$$

We define a two-time covariance $\Sigma_q(t, t+\tau)$,

$$\Sigma_q(t, t+\tau) := \langle [q'(t) - q(t)]\,[q'(t+\tau) - q(t+\tau)] \rangle\,. \tag{20}$$

Note that we stick to steady-state so that $\Sigma_q(t, t+\tau)$ is determined by only $\tau$. The Fourier transform of $\Sigma_q(t, t+\tau)$ is defined as,

$$C_q(\omega) := \int_{-\infty}^{+\infty} d\tau \Sigma_q(t, t+\tau) e^{i\omega\tau}. \tag{21}$$

MSE of the position estimation, $\Pi_q$, is given as as,

$$\Pi_q := \Sigma_q(t,t) = \int_{-\infty}^{+\infty} \frac{d\omega}{2\pi} C_q(\omega). \tag{22}$$

Our aim is to derive the filter $\tilde{J}_q(\omega)$ minimizing $\Pi_q$ and obtain the least $\Pi_q$.

Let's focus on $C_q(\omega)$ because $\Pi_q$ is minimized by minimizing $C_q(\omega)$ at all the $\omega$. After some algebra, we find the following:

$$C_q(\omega) = \left|\tilde{J}_q(\omega) g_{\varphi q}(\omega) - 1\right|^2 S_q(\omega) + \left|\tilde{J}_q(\omega)\right|^2 S_z(\omega), \tag{23}$$

where $S_k(\omega)$ is a spectral density defined as $S_k(\omega) = \int_{-\infty}^{+\infty} d\tau \langle k(t)k(t+\tau)\rangle e^{i\omega\tau}$ $(k = q, z)$. By setting $\partial C_q(\omega)/\partial \tilde{J}_q(\omega) = 0$, we obtain the optimal position filter $\tilde{J}_q^{\rm opt}(\omega)$,

$$\tilde{J}_q^{\rm opt}(\omega) = \frac{g_{\varphi q}^*(\omega) S_q(\omega)}{|g_{\varphi q}(\omega)|^2 S_q(\omega) + S_z(\omega)}. \tag{24}$$

Accordingly, the least MSE is derived as,

$$\Pi_q^{\rm min} = \int_{-\infty}^{+\infty} \frac{d\omega}{2\pi} \left( \frac{1}{S_q(\omega)} + \frac{|g_{\varphi q}(\omega)|^2}{S_z(\omega)} \right)^{-1}. \tag{25}$$

The other optimal filters and MSEs for $p$ and $f$ can be obtained by changing the subscript $q$ to $p$ or $f$.

The spectral densities $S_k(\omega)$ $(k = q, p, f, z)$ in our experiment are obtained as follows: First, $S_z(\omega)$ is easily obtained from Eq. (14),

$$S_z(\omega) = \frac{\bar{R}_{\rm sq}}{4|\alpha|^2}. \tag{26}$$

The external force $f(t)$ obeys the Ornstein-Uhlenbeck process,

$$\frac{df(t)}{dt} = -\lambda f(t) + w(t), \tag{27}$$

$$\langle w(t)w(\tau)\rangle = \kappa\delta(t-\tau). \tag{28}$$

Thus, $S_f(\omega)$ is given as,

$$S_f(\omega) = \frac{\kappa}{\omega^2 + \lambda^2}. \tag{29}$$

Other spectral densities can be calculated by using the relation $S_i(\omega) = |g_{ij}(\omega)|^2 S_j(\omega)$. From Eq. (6) we obtain,

$$S_q(\omega) = |g_{qf}(\omega)|^2 S_f(\omega) = \left|\frac{T_0(\omega)}{G\beta}\right|^2 \frac{\kappa}{\omega^2+\lambda^2}, \tag{30}$$

$$\begin{aligned} S_p(\omega) &= |g_{pf}(\omega)|^2 S_f(\omega) = |g_{pq}(\omega) g_{qf}(\omega)|^2 S_f(\omega) \\ &= (m\omega)^2 \left|\frac{T_0(\omega)}{G\beta}\right|^2 \frac{\kappa}{\omega^2+\lambda^2}. \end{aligned} \tag{31}$$

## IV. PHOTON FLUX FLUCTUATION

In this section, we will derive the spectral density of the photon flux fluctuation $S_{\Delta I}(\omega)$ and discuss the validity of the approximation used in the main text, $S_{\Delta I}(\omega) \approx |\alpha|^2 e^{2r_{\rm p}}$.

In order to calculate the photon flux fluctuation, we use an annihilation operator for an electromagnetic field, $a(t)$, which satisfies the commutation relation [6],

$$\left[a(t), a^\dagger(t')\right] = \delta(t-t'), \tag{32}$$

$$[a(t), a(t')] = \left[a^\dagger(t), a^\dagger(t')\right] = 0. \tag{33}$$

Photon flux $I(t)$ and the mean photon flux $I_0$ are given as,

$$I(t) = a^\dagger(t)a(t), \tag{34}$$

$$I_0 = \langle I(t)\rangle\,. \tag{35}$$

We define the Fourier transform of an annihilation operator,

$$\tilde{a}(\omega) := \int_{-\infty}^{+\infty} dt a(t) e^{i\omega t}. \tag{36}$$

Note that this definition leads to $\tilde{a}^\dagger(\omega) = \tilde{a}(-\omega)$. The commutation relation in the frequency domain is derived from Eqs. (32) and (33),

$$\left[\tilde{a}(\omega), \tilde{a}^\dagger(\omega')\right] = 2\pi\delta(\omega-\omega'), \tag{37}$$

$$\left[\tilde{a}(\omega), \tilde{a}(\omega')\right] = \left[\tilde{a}^\dagger(\omega), \tilde{a}^\dagger(\omega')\right] = 0. \tag{38}$$

Spectral density of $a(t)$ is given as,

$$R(\omega) := \int_{-\infty}^{+\infty} d\tau \left\langle a^\dagger(t) a(t+\tau)\right\rangle e^{i\omega\tau} \tag{39}$$

$$= \int_{-\infty}^{+\infty} \frac{d\omega_1}{2\pi} \left\langle \tilde{a}^\dagger(\omega_1)\tilde{a}(\omega)\right\rangle. \tag{40}$$

The mean photon flux $I_0$ is obtained by integrating this spectral density $R(\omega)$,

$$I_0 = \int_{-\infty}^{+\infty} \frac{d\omega}{2\pi} R(\omega). \tag{41}$$

The spectral density of the photon flux fluctuation $S_{\Delta I}(\omega)$ is calculated as,

$$\begin{aligned} S_{\Delta I}(\omega) &= \int_{-\infty}^{+\infty} d\tau \left\langle (I(t)-I_0)\,(I(t+\tau)-I_0)\right\rangle e^{i\omega\tau} \\ &= \int_{-\infty}^{+\infty} \frac{d\omega_1 d\omega_2 d\omega_3}{(2\pi)^3} \left\langle \tilde{a}^\dagger(-\omega_1)\tilde{a}^\dagger(-\omega_3)\tilde{a}(\omega_2)\tilde{a}(\omega-\omega_3)\right\rangle \\ &+ \int_{-\infty}^{+\infty} \frac{d\omega}{2\pi} R(\omega) - \frac{\delta(\omega)}{2\pi}\int_{-\infty}^{+\infty} d\omega_1 d\omega_2 R(\omega_1)R(\omega_2). \end{aligned} \tag{42}$$

To derive $S_{\Delta I}(\omega)$, we have to calculate the fourth order moment of an annihilation operator. In our case, however, we use a Gaussian state (phase squeezed state), so the second order moment will suffice to describe $S_{\Delta I}(\omega)$.

Let's assume an annihilation operator of the form,

$$\tilde{a}(\omega) = 2\pi\delta(\omega)\,|\alpha| + \tilde{a}_{\rm sq}(\omega), \tag{43}$$

$$\begin{aligned} \tilde{a}_{\rm sq}(\omega) =& c_{1\rm a}(\omega)\tilde{a}_1(\omega) + c_{1\rm b}(\omega)\tilde{a}_1^\dagger(-\omega) \\ &+ c_{2\rm a}(\omega)\tilde{a}_2(\omega) + c_{2\rm b}(\omega)\tilde{a}_2^\dagger(-\omega), \end{aligned} \tag{44}$$

where $|\alpha|$ is a coherent amplitude, $\tilde{a}_{\rm sq}(\omega)$ represents the squeezing term ($\langle\tilde{a}_{\rm sq}(\omega)\rangle = 0$), $\tilde{a}_1(\omega)$ and $\tilde{a}_2(\omega)$ are vacuum modes. Here we set the amplitude as a real value without loss of generality. The expression of Eq. (44) is valid for any mean-zero Gaussian states including mixed states (i.e., squeezed thermal states), as long as the coefficient $c_{ij}(\omega)$ satisfies the following:

$$c_{ij}^*(\omega) = c_{ij}(-\omega), \tag{45}$$

$$|c_{1\rm a}(\omega)|^2 - |c_{1\rm b}(\omega)|^2 + |c_{2\rm a}(\omega)|^2 - |c_{2\rm b}(\omega)|^2 = 1, \tag{46}$$

$$\begin{aligned} &c_{1\rm a}^*(\omega)c_{1\rm b}(\omega) + c_{2\rm a}^*(\omega)c_{2\rm b}(\omega) \\ &- c_{1\rm a}(\omega)c_{1\rm b}^*(\omega) - c_{2\rm a}(\omega)c_{2\rm b}^*(\omega) = 0. \end{aligned} \tag{47}$$

Here these equations are imposed by the property of the Fourier transform and the commutation relation (Eqs. (37) and (38)).

To describe the photon flux fluctuation of the squeezed states, it is useful to define the quadrature operators,

$$x_{\rm sq}(\omega) := \frac{1}{2}\left[\tilde{a}_{\rm sq}(\omega) + \tilde{a}_{\rm sq}^\dagger(-\omega)\right], \tag{48}$$

$$p_{\rm sq}(\omega) := \frac{1}{2i}\left[\tilde{a}_{\rm sq}(\omega) - \tilde{a}_{\rm sq}^\dagger(-\omega)\right]. \tag{49}$$

Since we set the amplitude as a real value, $x_{\rm sq}$ ($p_{\rm sq}$) is the anti-squeezing (squeezing) quadrature. Photon flux spectrum (except the amplitude contribution), squeezing spectrum and anti-squeezing spectrum (spectral densities of $\tilde{a}_{\rm sq}(\omega)$, $p_{\rm sq}(\omega)$ and $x_{\rm sq}(\omega)$) are given as,

$$R_{\rm sq}^I(\omega) = \int_{-\infty}^{+\infty}\frac{d\omega_1}{2\pi}\left\langle \tilde{a}_{\rm sq}^\dagger(\omega_1)\tilde{a}_{\rm sq}(\omega)\right\rangle, \tag{50}$$

$$R_{\rm sq}^-(\omega) = \int_{-\infty}^{+\infty}\frac{d\omega_1}{2\pi}\left\langle p_{\rm sq}^\dagger(\omega_1)p_{\rm sq}(\omega)\right\rangle, \tag{51}$$

$$R_{\rm sq}^+(\omega) = \int_{-\infty}^{+\infty}\frac{d\omega_1}{2\pi}\left\langle x_{\rm sq}^\dagger(\omega_1)x_{\rm sq}(\omega)\right\rangle. \tag{52}$$

Here squeezing and anti-squeezing spectrum satisfy an uncertainty principle, $R_{\rm sq}^+(\omega)R_{\rm sq}^-(\omega) \geq 1/16$ ($\hbar = 1/2$). From Eqs. (43) $\sim$ (52), we obtain,

$$\begin{aligned} R_{\rm sq}^\pm(\omega) =& \frac{1}{4}\left|c_{1\rm a}(\omega) \pm c_{1\rm b}(\omega)\right|^2 \\ &+ \frac{1}{4}\left|c_{2\rm a}(\omega) \pm c_{2\rm b}(\omega)\right|^2, \end{aligned} \tag{53}$$

$$R_{\rm sq}^I(\omega) = R_{\rm sq}^+(\omega) + R_{\rm sq}^-(\omega) - \frac{1}{2}. \tag{54}$$

Then, after some algebra, Eq. (42) is rewritten as,

$$\begin{aligned} S_{\Delta I}(\omega) =& 4|\alpha|^2 R_{\rm sq}^+(\omega) \\ &+ \int_{-\infty}^{+\infty}\frac{d\omega_1}{2\pi}\left[2R_{\rm sq}^+(\omega_1+\omega)R_{\rm sq}^+(\omega_1) - \frac{1}{8}\right] \\ &+ \int_{-\infty}^{+\infty}\frac{d\omega_1}{2\pi}\left[2R_{\rm sq}^-(\omega_1+\omega)R_{\rm sq}^-(\omega_1) - \frac{1}{8}\right]. \end{aligned} \tag{55}$$

Next, we will assume that the squeezed state has finite bandwidth, and then verify the approximation used in the main text.

Let's consider the squeezing spectrums $R_{\rm sq}^\pm(\omega)$ of the standard form [1, 2],

$$R_{\rm sq}^\pm(\omega) = \frac{1}{4} + \left(R_{\rm sq}^\pm(0) - \frac{1}{4}\right)\frac{(\Delta\omega_\pm)^2}{\omega^2 + (\Delta\omega_\pm)^2}, \tag{56}$$

$$\frac{\Delta\omega_+}{\Delta\omega_-} = \sqrt{\frac{1-4R_{\rm sq}^-(0)}{4R_{\rm sq}^+(0)-1}}, \tag{57}$$

where $\Delta\omega_-$ ($\Delta\omega_+$) is the bandwidth of squeezing (anti-squeezing), the second equation ensures that $R_{\rm sq}^+(\omega)R_{\rm sq}^-(\omega) = 1/16$ for all $\omega$ when the squeezed state is pure. Here we define the averaged squeezing bandwidth $\Delta\omega_0$ and the squeezing parameters ($r_{\rm m}$, $r_{\rm p}$) at the center frequency ($\omega = 0$) as,

$$\Delta\omega_0 := \frac{1}{2}\left(\Delta\omega_- + \Delta\omega_+\right), \tag{58}$$

$$e^{-2r_{\rm m}} := 4R_{\rm sq}^-(0), \tag{59}$$

$$e^{2r_{\rm p}} := 4R_{\rm sq}^+(0). \tag{60}$$

In the case of the OPO, $\Delta\omega_0$ corresponds to the half width at half maximum of the OPO.

By inserting Eq. (56) to Eq. (55), we obtain,

$$\begin{aligned} S_{\Delta I}(\omega) =& 4|\alpha|^2 R_{\rm sq}^+(\omega) + I_{\rm sq} \\ &+ \frac{1}{8}\left[\frac{(e^{2r_{\rm p}}-1)^2(\Delta\omega_+)^3}{\omega^2 + (2\Delta\omega_+)^2} + \frac{(1-e^{-2r_{\rm m}})^2(\Delta\omega_-)^3}{\omega^2 + (2\Delta\omega_-)^2}\right], \end{aligned} \tag{61}$$

$$\begin{aligned} I_{\rm sq} :=& \int_{-\infty}^{+\infty}\frac{d\omega}{2\pi}R_{\rm sq}^I(\omega) \\ =& \frac{1}{8}\left[(e^{2r_{\rm p}}-1)\Delta\omega_+ + (e^{-2r_{\rm m}}-1)\Delta\omega_-\right], \end{aligned} \tag{62}$$

where $I_{\rm sq}$ is the mean photon flux of the squeezing ($I_0 = |\alpha|^2 + I_{\rm sq}$).

If the averaged squeezing bandwidth $\Delta\omega_0$ is much larger than the system parameters, i.e., $\Delta\omega_0 \gg \Omega, \lambda$ ($\Omega$: the resonant frequency of the mirror, $\lambda$: the cutoff frequency of the external force), we may assume $\omega \ll \Delta\omega_\pm$. Note that we implicitly assume that $\Delta\omega_0 \sim \Delta\omega_- \sim \Delta\omega_+$, which would be justified in our experimental situation as described later. The photon flux fluctuation $S_{\Delta I}(\omega)$ would be approximated to,

$$S_{\Delta I}(\omega) \simeq \left(|\alpha|^2 + \xi I_{\rm sq}\right) e^{2r_{\rm p}}, \tag{63}$$

$$\xi := e^{-2r_{\rm p}} \left(1 + \frac{1}{4} \frac{(e^{2r_{\rm p}} - 1)^{3/2} + (1 - e^{-2r_{\rm m}})^{3/2}}{\sqrt{e^{2r_{\rm p}} - 1} - \sqrt{1 - e^{-2r_{\rm m}}}}\right), \tag{64}$$

where the parameter $\xi$ ranges from 1 ($r_{\rm p} = r_{\rm m} = 0$) to 1/4 ($r_{\rm p} \to \infty$). If $\xi I_{\rm sq} \ll |\alpha|^2$,

$$S_{\Delta I}(\omega) \approx |\alpha|^2 e^{2r_{\rm p}}. \tag{65}$$

Let's consider whether these conditions ($\Delta\omega_0 \gg \Omega, \lambda$ and $\xi I_{\rm sq} \ll |\alpha|^2$) are satisfied under our experimental situation. The experimental parameters are, $e^{2r_{\rm p}} = 3.98$ (6.00 dB), $e^{-2r_{\rm m}}$=0.435 ($-3.62$ dB), $\xi = 0.61$, $\Delta\omega_+/\Delta\omega_- = 0.435$, $\Omega = 1.76 \times 10^5$ rad/s, and $\lambda = 5.84 \times 10^4$ rad/s. The averaged squeezing bandwidth $\Delta\omega_0$, however, is tricky to determine. As in Ref. [1], we utilize only finite bandwidth around a sideband frequency of 5 MHz. Thus it is not appropriate to define the squeezing bandwidth $\Delta\omega_0$ as an OPO's bandwidth ($\Delta\omega_{\rm OPO} = 8.2 \times 10^7$ rad/s ). We should consider an effective squeezing bandwidth $\Delta\omega_0^{\rm eff}$ which is not unnecessarily large, but still satisfies $\Delta\omega_0^{\rm eff} \gg \Omega, \lambda$.

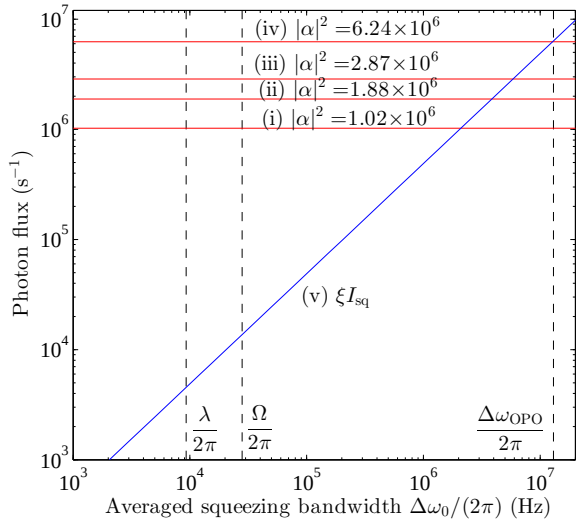


FIG. 3: Photon flux versus averaged squeezing bandwidth. Lines (i) to (iv) represent the amplitude squares $|\alpha|^2$ used in the experiment. Trace (v) is the scaled photon flux of squeezing, $\xi I_{\rm sq}$, which is calculated from Eqs. (62) and (64). Dashed lines show the specific frequencies in the experiment, $\lambda$, $\Omega$, $\Delta\omega_{\rm OPO}$.

Figure 3 shows $\xi I_{\rm sq}$ as a function of the squeezing bandwidth $\Delta\omega_0$. We also plot experimental amplitude squares $|\alpha|^2 = 1.02, 1.88, 2.87, 6.24 \times 10^6$ s$^{-1}$. In Fig. 3, there is a certain region which satisfies $\Delta\omega_0 > \Omega, \lambda$ and $\xi I_{\rm sq} < |\alpha|^2$. For example, let's set the effective squeezing bandwidth as ten times of the resonant frequency, $\Delta\omega_0^{\rm eff} = 10\Omega$ ($> 10\lambda$). In this case, we obtain $\xi I_{\rm sq} = 1.37 \times 10^5$ s$^{-1}$ which is still an order smaller than the experimental $|\alpha|^2$. Thus we can assume the effective squeezing bandwidth which simultaneously satisfies $\Delta\omega_0^{\rm eff} \gg \Omega, \lambda$ and $\xi I_{\rm sq} \ll |\alpha|^2$. Accordingly we may conclude that the approximation $S_{\Delta I}(\omega) \approx |\alpha|^2 e^{2r_{\rm p}}$ is valid within our experimental conditions.

[1] H. Yonezawa, D. Nakane, T. A. Wheatley, K. Iwasawa, S. Takeda, H. Arao, K. Ohki, K. Tsumura, D. W. Berry, T. C. Ralph, H. M. Wiseman, E. H. Huntington, and A. Furusawa, Science **337**, 1514-1517 (2012).

[2] Y. Takeno, M. Yukawa, H. Yonezawa, and A. Furusawa, Opt. Express **15**, 4321-4327 (2007).

[3] T. A. Wheatley, D. W. Berry, H. Yonezawa, D. Nakane, H. Arao, D. T. Pope, T. C. Ralph, H. M. Wiseman, A. Furusawa, and E. H. Huntington, Phys. Rev. Lett. **104**, 093601 (2010).

[4] H. L. Van Trees, *Detection, Estimation, and Modulation Theory, Part I* (Wiley, New York, 2001).

[5] D. W. Berry and H. M. Wiseman, Phys. Rev. A **65**, 043803 (2002).

[6] C. W. Gardiner, P. Zoller, *Quantum Noise* (Springer, 2000).